Essential constraints for detecting deep sources in EEG - application to orthostatic tremor

Muthuraman M, Deuschl G, and Raethjen J

Department of Neurology, Christian Albrechts University

Kiel, Germany

Abstract—**The hypotheses that orthostatic tremor is generated by a central oscillator is been tested in this paper. In order to understand the mechanisms of the central network its sources need to be found. The cortical sources of both the basic and first "harmonic" frequency of orthostatic tremor are addressed in this paper. The Dynamic Imaging of Coherent Sources (DICS) was used to find the coherent sources in the brain. The three essential constraints for detecting deep sources in the brain using EEG data were tested by three model simulations. The optimal number of electrodes, length of the data and the signal to noise ratio required for error-free localization was tested. In all the orthostatic tremor patients the corticomuscular coherence was also present in the basic and the first harmonic frequency of the tremor. The basic frequency constituted a network of primary leg area, supplementary motor area, primary motor cortex, two pre-motor sources, diencephalon and cerebellum. The first harmonic frequency was in the region of primary leg area, supplementary motor area, primary motor cortex, diencephalon and cerebellum. Thus the generation of these two oscillations involves the same network structure and indicates the oscillation at double the tremor frequency is a harmonic of the basic tremor frequency. The orthostatic tremor could have the central oscillator in the brain.**

Keywords-DICS; Orthostaic tremor; SNR; EEG; Simulation

I. INTRODUCTION

Orthostatic tremor (OT) is a motor disorder which involves legs and trunk when standing upright and is relieved during walking and sitting [1, 2]. This tremor is accompanied by a characteristic 13-18 Hz bursting EMG pattern [3]. The mechanisms underlying OT is still unknown. The involvement of the central nervous system is commonly assumed [4-6]. A number of studies have suggested possible supraspinal sites as the origin of the activity [7] including the brain stem [8], the motor cortex [9] and the pons and cerebellum [10] but no single site has emerged as the origin of this tremor. In the present paper we use dynamic imaging of coherent sources (DICS) which applies a spatial filter to localize brain activity that is coherent with a peripheral tremor signal [11]. The three essential constraints which are tested in this study with two simulations are the dependency on number of channels, length of the data and the signal to noise ratio (SNR) of the available data. The dependencies on number of channels are extensively studied in other source algorithms [12]. The three constraints were tested on MEG data using DICS to test the spatial resolution in [13]. The third simulation was done to test the accuracy of the analysis for an extended cortical activity. But, all these constraints were tested in this work for attaining a error free localization of deep sources. In this study, we look for the sources of the basic frequency and double the tremor frequency separately by applying DICS and having the EMG as reference signal in all runs of the source analysis.

II. METHODS

A. Source Analysis

The basis of the source analysis (DICS) [11] is the so-called beamforming approach [13, 14]. The output of a beamformer at a location q of interest can be defined as a weighted sum of the output of all (E_n) signal channels [15], or expressed mathematically as:

$$B = W \bullet E_f \tag{1}$$

where B is the beamformer output with source strength in nAm, W is the $1 \times E_n$ weight vector for a given direction of the source at the target location, and E_f is the $E_n \times \delta$ matrix of the electric field at the electrode locations at all (δ) latencies. The weights determine the spatial filtering characteristics of the beamformer and are designed to increase the sensitivity to signals from a location of interest and reducing the contribution of the signals from (noise) sources at different locations. The beamformer weights for a source at a location of interest are determined completely by the data covariance matrix and the forward solution (leadfield L_f) for the target source [15]. The frequency components and their linear interaction are represented as a cross-spectral density matrix $(E_n \times E_n \times F)$; E_n - number of EEG electrodes, F - number of frequency bins. The two measures which can be derived from the cross spectral density matrix are power and coherence. Coherence can be

estimated by normalizing the cross spectral density between two signals with their power spectral densities. Inorder to image power and coherence in the brain at a given frequency range, a linear transformation is used based on a constrained optimization problem which acts a spatial filter [15]. The transformation is attained by minimizing the variance of the output of the spatial filter while constraining the filter such that the activity of the source at position q is passed with unity gain:

$$\min[\xi\{\|S_a D\|^2\} + R_\alpha \|S_a\|] \text{ subject to} \quad (2)$$

$$S_a L_f(q) = I \quad (3)$$

where ξ is the expectation value, S_a the linear transformation matrix which is the spatial filter, D is the Fourier transformed data, I is the unit matrix, and R_α the regularization parameter. The columns of $L_f(q)$ contains the solution of the forward problem for two orthogonal radial unit dipoles at location q. In a spherical conductor, such dipoles span the space containing all possible source orientations that can be detected by EEG. The regularization parameter is expressed relative to the largest eigenvalue of $C_s(f)$, where $C_s(f)$ is the cross spectral density at a specific frequency bin or range, i.e., $R_\alpha = \gamma_{\max} R'_\alpha$, where $\gamma_{\max}$ is the largest eigenvalue of $C_s(f)$ and R'_α is the relative regularization. The frequency-dependent solution of the above equation is

$$S_a(q,f) = (L_f^T(q) C_s^q(f)^{-1} L_f(q))^{-1} L_f^T(q) C_s^q(f)^{-1} \quad (4)$$

where $C_s^q(f) = C_s(f) + R_\alpha I$. The cross spectrum between the radial source combinations at the two locations (q_1, q_2) can then be obtained as:

$$C'_s(q_1, q_2, f) = S_a(q_1, f) C_s(f) S_a^{*T}(q_2, f). \quad (5)$$

In the case, when $q_1 = q_2$, C'_s represents the estimate of signal power at each location. If the singular values of C'_s fulfill $\gamma_1 >> \gamma_2$ the cross spectrum, and thus both the estimates coherence and power can be attributed to sources with fixed orientations. If the singular value relation does not hold, power and coherence estimates can be obtained using the trace of the matrix $C'_s(q_1, q_2, f)$. The singular value relation also provides an alternative approach in which the coherence estimation may be limited to the sources which have a fixed orientation. This assumption is also well understood in neurophysiology as detection of neuronal events with EEG requires simultaneous activation of thousands of pyramidal cells in a small cortical area, with the perpendicular orientation of their apical dendrites allowing summation of neural currents. Sources with a prominent, dominant direction of current flow are thus more likely to represent accurate localization of a focal functional area than sources with no preferred direction. By using the beamforming techniques one can obtain an estimate of the signals originating from any given location in the brain [15]. The beamformer estimation is performed with a grid spacing of 5 mm covering the entire brain. The entire brain is divided into 3560 rectangular grids called voxels. The DICS tomographic maps are formed by calculating the power and coherence estimates at all grid points and overlaying them on the individual or the standard anatomical magnetic resonance images. The reference signal used in coherence calculation can be either an external signal like the EMG or the beamformer estimate of activity originating from a selected cortical area in the brain. Power maps are presented as power statistical maps using SPM software and the 99% confidence level for coherence can be calculated using surrogate data as described in [17]. After, identifying the brain areas, their time series can be derived using the spatial filter [15].

B. Model Simulation

The three essential constraints number of channels, SNR and length of the data for a good source localisation using the DICS were tested using simulations. Finally, when there is distributed activity in the scalp EEG does the source analysis automatically locate deep sources in the centre of the brain. Simulations are a useful way to test the limitations of the method.

The first essential constraint which was tested using the simulations is the number of EEG channels required for a good source localisation using DICS. The dependency of the source analysis algorithms on the number of channels is extensively studied on other algorithms [12]. The simulations were done by means of creating a time series of current dipoles for each voxel in the data set and then calculate the corresponding EEG signal. After that, it is possible to calculate the inverse solution of these EEG signals and compare them with the generated data. In all the simulations the data was generated using the five-concentric-spheres model. The second and the third constraint of SNR and the length of the data were combined and tested in the second simulation. All three constraints were studied in DICS with simulations on MEG data [13] to test the spatial resolution and not to test the minimum length and SNR required for error free localization of deep sources.

The last simulation was based on the fact when there is distributed activity on the scalp EEG. In orthostatic tremor all the channels are highly coherent with the reference EMG signal. In this case, the source analysis is able to locate meaningful sources on the cortical and sub cortical level. This situation was also tested using a simulation on the cortical level.

In the **first simulation**, the data is generated by assuming an autoregressive (AR) process of order two defined as:

$$y(t) = a_1 y(t-1) + a_2 y(t-2) + \eta(t) \qquad (6)$$

where a_1 and a_2 are the AR2 coefficients and $\eta(t)$ is the white Gaussian noise with zero mean and unit variance, as the sources in two (active) voxels. The poles in the complex plane for the AR2 process were both 0.99, i.e., $a_1 = 1.971$ and $a_2 = -0.9801$ are the AR2 coefficients for a 15Hz process. The first issue of number of EEG channels required to get accurate source localization on the cortical level was tested.

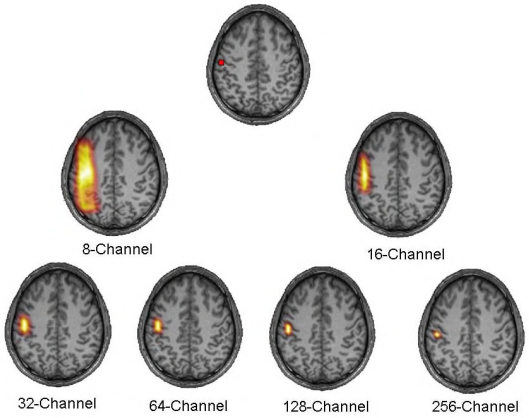

Figure 1. The simulated voxel is highlighted in red in the first slice followed by the results of the different channel configuration from 8 channels to 256 channels.

In step1 the source for the 15 Hz was implemented in one active voxel in the cortex contralateral (C) to the assumed muscle is the voxel number 3426. The "EEG signal" was produced with a broad-band AR2 plus white noise of 25 % (SNR= 4 dB) (compared to the clean 15 Hz AR2 signal "of infinite SNR") was added to the other voxels. The CMC source is marked in red in Fig. 1. The reference EMG signal was the 15Hz AR2 process with added broad band noise to tune the coherence to 0.8 (as seen in real data). The forward modeling was done by assuming different channel configuration starting from 8-channels to 256 channels. The difference in location of sources was drastically changed from 8-channels to 32-channels. But, by increasing the number of channels above 32 gives only a better spatial resolution in locating the source can be seen from Fig.1. The optimal range for the number of channels using this simple simulation is 32 channels.

In the **second simulation**, the EEG data was generated as in the first simulation but this time there were two active voxels one in the CMC as the previous simulation and the other active voxel in the diencephalon voxel number 526. The length of the data was simulated from 1 second to 5 seconds insteps of one second, after 5 seconds till 200 seconds insteps of 5 seconds. Because the main aim of this simulation is to locate the sources with less location error in the cortical and sub-cortical level with lesser length of data. The level of SNR was varied from 10 dB to 30 DB in steps of 5 dB. Each simulation step was repeated 10 times. The location error was calculated by taking the difference between the identified and the simulated voxel. The mean location error for all the 10 simulations was calculated and indicated as percentage in Fig. 2 A for the CMC source and the Fig 2.B for the diencephalon source. In fig 3.C and 3.D the mean coherence at the frequency 15 Hz between the spatially filtered source signal and the reference signal is depicted. This simulation indicated that 5 seconds of data and the SNR should be 30 dB is the optimal range for the source analysis for good source localization in cortical and sub-cortical level.

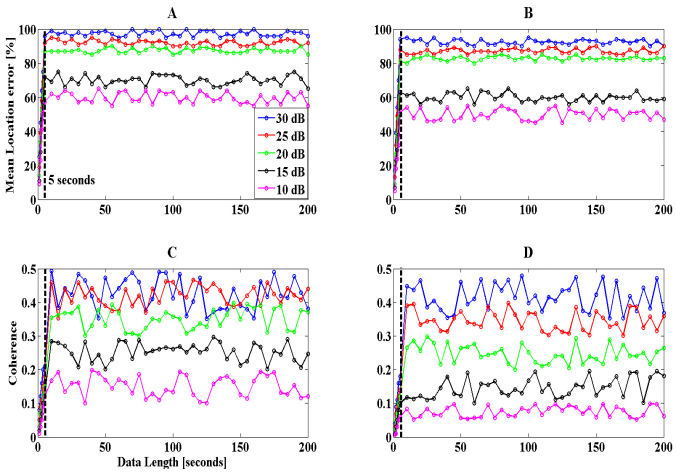

Figure 2. A. The mean location error (accuracy) in percentage for the different SNR's is plotted for the CMC source. B. The mean location error (accuracy) in percentage for the different SNR's is plotted for the diencephalon source C. The mean coherence value at 15 Hz between the spatially filtered source signal and the reference signal for the CMC source. D. The mean coherence for the diencephalon source.

In the **third simulation**, the EEG was generated by making all the cortical voxels active which overlay only on the grey matter with a 15Hz Ar2 process. The activated voxels are shown in red in Fig. 3 A in an axial slice.

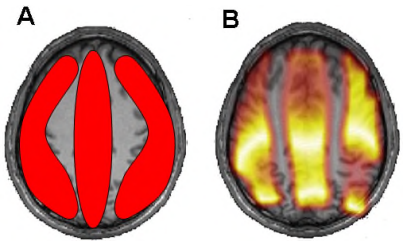

Figure 3 A. The simulated voxels which overlay on the grey matter is highlighted in red in an axial slice B. The result is shown as a grand average of all the 10 simulations in a single axial slice.

This simulation was repeated 10 times with different independent noises for generating the AR2 process. The primary goal was to investigate whether the simulated extended cortical activity has a default midline sub-cortical source (e.g. Thalamus) in the brain. But, the source analysis detected only the extended cortical activity and no additional source in the sub-cortical level. The result of all the 10 simulations is shown as grand average in Fig. 3 B on an axial slice.

III. Application to Orthostatic Tremor Patients

The DICS method was applied to 6 OT patients all of whom had clear peaks in the power spectrum, and coherence spectrum at the basic and first harmonic frequency. The average basic frequency for all the patients was 15.5 Hz and the average first harmonic frequency was 30.4 Hz.

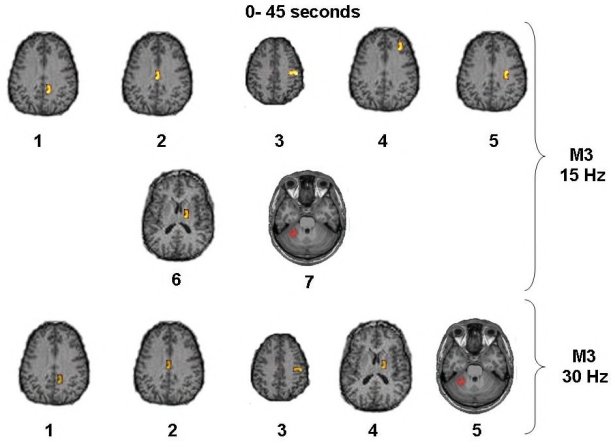

Figure 4. The single slice plots showing all the active sources for the basic frequency and the first harmonic frequency in an orthostatic tremor patient.

In all the patients the source for the basic frequency and the first harmonic frequency was found in the contralateral side of the brain as to be seen in the example of Fig. 4 in the slice plot with twelve slices of the brain. For this example patient the anterior tibial muscle on the left leg was taken as the reference. The repetitive runs of the source analysis identified almost similar network responsible for both the basic and first harmonic frequency of this tremor. The locations for the basic frequency comprise the Primary leg area, supplementary motor area (SMA), primary motor area, two pre-motor sources, diencephalon and cerebellum as shown in Fig. 4 on single slices for each source separately. The two frequencies in these patients have almost identical origins in the brain indicating that they are likely simple harmonics and do not reflect separate oscillations as in the Parkinsonian patients [18]. The next important result is that in OT is the involvement of cerebellum which can be seen in Fig.4. This data clearly show that OT originates from central networks in the brain.

IV. Conclusion

In conclusion, the first model simulation showed us that 32 EEG electrodes are required to locate a simulated cortical source without any error in location. Using the second simulation we were able to identify the minimum length of data required for identifying cortical and sub-cortical sources are 5 seconds with a SNR of 30 dB. The third simulation proved that the DICS does not locate any ghost sources in the sub-cortical areas when there is extended cortical activity. The application of DICS to orthostatic tremor revealed the complete network for the basic tremor frequency and the first harmonic frequency which are not different in there network structure and they are not independent oscillations as in the case of Parkinson's disease [18].

Acknowledgment

Support from the German Research Council (Deutsche Forschungsgemeinschaft, DFG, SFB 855, Project D2) is gratefully acknowledged.

References

[1] K. M. Heilmann, "Orthosatic tremor", Arch Neurol 41, 1984, pp.880-881.

[2] P. D. Thompson, J. C. Rothwell, B. L. Day, A. Berardelli, J. P. R. Dick, C. D. Marsden, "The physiology of orthostatic tremor", Arch Neurol 239, 1986, pp.209-217.

[3] B. Boroojerdi, A. Ferbert, H. foltys, C. M. Kosinski, M. Schwarz, "Evidence for a non-othostatic tremor", J. Neurol Neurosurg. Psychiatry. 66, 1999, pp.284-288.

[4] P.D Thompson, J. C. Rothwell, B. L. Day et al, "The physiology of orthostatic tremor", Arch Neurol 239, 1986, pp.584-587.

[5] T. C. Britton, P. D. Thompson, W. vsn der Kamp et al, "Primary orthostatic tremor: further observations in six cases", J. Neurol 239, 1992, pp.209-217.

[6] G. Deuschl, C. H. Lucking, J. Quintern, "Orthostatic tremor: clinical aspects, pathophysiology and therapy", EEG and EMG Z Elektoenzephalogr Elektromyogr Verwandte Geb 18, 1996, pp.13-19.

[7] J. H. McAuley, T. C. Briston, J. Rothwell, L. J. Findley, C. D.Marsden, "The timing of primary orthostatic tremor bursts has a task-specific plasiticity", Brain 123, 2000, pp.254-266.

[8] Y. R. Wu, P. Ashby, A. E. Lang, "Orthostatic tremor arises from an oscillator in the posterior fossa", Mov. Disord 16, 2001, pp.272-279.

[9] C. H. Tsai, J. G. Semmler, T. e. Kimber et al, "Modulation of primary orthostatic tremor by magnetic stimulation over the motor cortex", J. Nuerol Neurosurg Pyschiatry 64, 1998, pp. 33-36.

[10] J. Benito-Leon, J. Rodriguez, M. Orti-Pareja, L. Ayuso-Peralta, F. J. Jimenez-Jimenez, J.A Molina, "Symptomatic orthostatic tremor in pontine lesions", Neurology 49, 1997, pp. 1439-1441.

[11] J. Gross, "Dynamic imaging of coherent sources: Studying neural interactions in the human brain" PNAS 98, .2001, pp.694-699.

[12] C. M. Michel, M. M. Murray, G. Lantz, S. Gonzalez, L. Spinelli, R. Grave de Peralta, "EEG source imaging", Clin. Neurophysiol. 115 (10), 2004, pp.2195-2222.

[13] A. Hillebrand, K. D. Singh, L. E. Holliday, P. L. Furlong, G. R. Barnes, "A new approach to neuroimaging with magnetoencephalography", Hum. Brain Mapp. 25, 2005, pp. 199-211.

[14] K. Sekihara, B. Scholz, "Generalized Wiener estimation of three-dimensional current distribution from biomagnetic measurements", IEEE Trans. Biomed. Eng. 43, 1996, pp. 281-291.

[15] B. D Van Veen, W. V. Drongelen, M. Yuchtmann, A. Suzuki, "Localization of brain electrical activity via linearly constrained minimum variance spatial filtering", IEEE Trans. Biomed. Eng. 44, 1997, pp. 867-880.

[16] J. Gross, L. Timmermann, J. Kujala, R. Salmelin, R, Schnitzler A, "Properties of MEG tomographic maps obtained with spatial filtering", Neuroimage 19(4), 2003, pp.1329-1336.

[17] M. Priestley, "Spectral analysis and time series", Academic Press, New York, 1981, 890p.

[18] M. Muthuraman, J. Raethjen, H. Hellriegel, G. Deuschl, U. Heute, "Imaging coherent sources of tremor related EEG activity in patients with Parkinson's disease", IEEE EMBC, 2008, 113 (5), pp.4716-4719.